inorganics

MDPI

Communication

Heteroleptic Zn(II)–Pentaiodobenzoate Complexes: Structures and Features of Halogen–Halogen Non-Covalent Interactions in Solid State

Mikhail A. Bondarenko [1], Alexander S. Novikov [2,3], Maxim N. Sokolov [1] and Sergey A. Adonin [1,*]

[1] Nikolaev Institute of Inorganic Chemistry SB RAS, Lavrentieva St., 3, 630090 Novosibirsk, Russia
[2] Institute of Chemistry, Saint Petersburg State University, Universitetskaya Nab., 7/9, 199034 Saint Petersburg, Russia
[3] Research Institute of Chemistry, Peoples' Friendship University of Russia, Miklukho-Maklaya St., 6, 117198 Moscow, Russia
* Correspondence: adonin@niic.nsc.ru

Abstract: Reactions between Zn(II) nitrate, pentaiodobenzoic acid (HPIBA) and different pyridines in dimethylformamide (DMF) result in the formation of the heteroleptic neutral complexes [Zn(3,5-MePy)$_2$PIBA$_2$] (**1**) and [Zn(DMF)$_3$(NO$_3$)PIBA] (**2**). Both compounds were isolated in pure form, as shown by the PXRD data. The features of specific non-covalent interactions involving halogen atoms (halogen bonding) were examined by means of DFT calculations (QTAIM analysis and the estimation of corresponding energies).

Keywords: zinc complexes; carboxylates; non-covalent interactions; polyhalogenated arenes; halogen bonding

Citation: Bondarenko, M.A.; Novikov, A.S.; Sokolov, M.N.; Adonin, S.A. Heteroleptic Zn(II)–Pentaiodobenzoate Complexes: Structures and Features of Halogen–Halogen Non-Covalent Interactions in Solid State. *Inorganics* **2022**, *10*, 151. https://doi.org/10.3390/inorganics10100151

Academic Editor: Michael A. Beckett

Received: 25 August 2022
Accepted: 16 September 2022
Published: 22 September 2022

1. Introduction

Complexes with halogen-polysubstituted organic (in particular, aromatic) ligands constitute a not very large, but important and interesting, field of coordination chemistry. The lion's share of them are those containing perfluorinated substituents [1–8], mostly due to their potential applications in luminescent materials [8–12] (it is commonly assumed that the replacement of protons by F reduces quenching [13]). At the same time, the ligands polysubstituted by other halogens are much less studied. Here, we give some examples illustrating this current misbalance. Pentachlorobenzoic acid has been known about since at least 1887 [14] and, since then, authors have published optimized protocols of its quantitative preparation [15]; however, its structure was only reported in 2018 [16], and there is only one article on the corresponding structurally characterized complex [17]. Works on ligands with heavier halogens (especially iodine) are rare, despite the fact that some of these compounds—in particular, pentaiodobenzoic acid (HPIBA), known about for several decades [18]—can be of interest in terms of design of contrast media for tomography (a very interesting paper demonstrating the potential of this pathway was recently presented by Lin et al. [19]).

A few years ago, we performed structural characterization of HPIBA and its several salts, [20] noting that it features very strong (as shown by the DFT calculation) halogen bonding (XB) [21–23]. We assumed that this feature must also persist in hypothetic PIBA metal complexes. Soon after, we reported the first examples of such compounds (heteroleptic Cu(II) PIBA complexes [24]), and an analysis of the corresponding structural data confirmed our hypothesis.

Continuing this work, we hereby present the first PIBA complexes of Zn(II)—[Zn(3,5-MePy)$_2$PIBA$_2$] (**1**) and [Zn(DMF)$_3$(NO$_3$)PIBA] (**2**). Both of these compounds were characterized using X-ray diffractometry and obtained as pure phases (as shown by the PXRD

data). The features of non-covalent interactions in both crystal structures were investigated by means of DFT calculations.

2. Materials and Methods

All reagents were obtained from commercial sources and used as purchased. HPIBA was synthesized according to the previously published procedure [18].

2.1. Synthesis of 1

A total of 80 mg (0.106 mmol) of HPIBA was dissolved in 2 mL of DMF, followed by addition of 24 μL (0.212 mmol) of 3,5-MePy and solution of 16 mg (0.053 mmol) of $Zn(NO_3)_2 \cdot 6H_2O$ in 1 mL of DMF. Slow diffusion of diethyl ether at r.t. (≈18 h) resulted in formation of transparent pale-yellow crystals of **1**. Yield, 79%. For $C_{28}H_{18}I_{10}N_2O_4Zn$, calcd %: C, 18.89; H, 1.02; and N, 1.57; found %: C, 19.01; H, 1.10; and N, 1.65. IR (4000–400 cm^{-1}, KBr): 1610 s, 1578 m, 1485 m, 1358 s, 1250 s, 1175 s, 1150 m, 1009 m, 859 m, 775 m and 695 s.

2.2. Synthesis of 2

A total of 120 mg (0.160 mmol) of HPIBA was dissolved in 2 mL of DMF, followed by addition of 30 μL (0.32 mmol) of 3-ClPy or equimolar amount of some other substituted pyridines (see Results and Discussion for details) and solution of 24 mg (0.08 mmol) of $Zn(NO_3)_2 \cdot 6H_2O$ in 1 mL of DMF. Slow diffusion of diethyl ether at r.t. (≈18 h) resulted in formation of transparent pale-yellow crystals of **1**. Yield, 84%. For $C_{16}H_{21}I_5N_4O_8Zn$, calcd %: C, 17.52; H, 1.93; and N, 5.11; found %: C, 17.69; H, 2.01; and N, 5.27.

2.3. X-ray Diffractometry

Crystallographic data and refinement details for **1** and **2** are given in Table 1. The diffraction data were collected using a Bruker D8 Venture diffractometer with a CMOS PHOTON III detector and IμS 3.0 source (Mo Kα radiation, λ = 0.71073 Å) at 150 K. The φ- and ω-scan techniques were employed. Absorption correction was applied via SADABS (Bruker Apex3 software suite, Apex3, SADABS-2016/2 and SAINT, version 2018.7-2; Bruker AXS Inc., Madison, WI, USA, 2017). Structures were solved via SHELXT [25] and refined via full-matrix least-squares treatment against $|F|^2$ in anisotropic approximation with SHELX 2014/7 [26] in ShelXle program [27]. H-atoms were refined in the geometrically calculated positions. The crystallographic data have been deposited in the Cambridge Crystallographic Data Centre under the deposition codes CCDC 2203477-2203478. These data can be obtained free of charge via www.ccdc.cam.ac.uk/data_request/cif, accessed on 24 August 2022 or by emailing data_request@ccdc.cam.ac.uk.

Table 1. XRD experimental details.

	(1)	**(2)**
Chemical formula	$C_{28}H_{18}I_{10}N_2O_4Zn$	$C_{16}H_{21}I_5N_4O_8Zn$
M_r	1780.81	1097.24
Crystal system, space group	Orthorhombic, *Fdd*2	Monoclinic, $P2_1/n$
α, β, γ (°)	90, 90, 90	90, 94.011 (1), 90
V (Å^3)	8048.2 (3)	2922.66 (10)
Z	8	4
μ (mm^{-1})	8.32	6.17
T_{min}, T_{max}	0.642, 0.746	0.616, 0.746
No. of measured, independent and observed [$I > 2\sigma(I)$] reflections	49,070, 6155, 6088	33,369, 5530, 5174

Table 1. *Cont.*

	(1)	(2)
R_{int}	0.029	0.030
θ values (°)	θ_{max} = 30.5, θ_{min} = 2.4	θ_{max} = 25.7, θ_{min} = 2.3
$(\sin\theta/\lambda)_{max}$ (Å^{-1})	0.715	0.610
Range of *h*, *k*, *l*	$h = -72 \rightarrow 72$, $k = -14 \rightarrow 14$, $l = -21 \rightarrow 21$	$h = -13 \rightarrow 13$, $k = -11 \rightarrow 11$, $l = -32 \rightarrow 32$
$R[F^2 > 2\sigma(F^2)]$, $wR(F^2)$, S	0.014, 0.036, 0.99	0.025, 0.058, 1.07
No. of reflections, parameters and restraints	6155, 204, 1	5530, 307, 0
$\Delta\rho_{max}$, $\Delta\rho_{min}$ (e Å^{-3})	0.74, −0.84	1.97, −1.20
Absolute structure	Flack x determined using 2891 quotients [(I+)−(I-)]/[(I+)+(I-)]	
Absolute structure parameter	0.000 (7)	

2.4. Powder X-ray Diffractometry

XRD analysis of polycrystals was performed using Shimadzu XRD-7000 diffractometer (CuK alpha radiation, Ni filter, linear One Sight detector, 0.0143° 2θ step, 2s per step). Plotting of PXRD patterns and data treatment were performed using X'Pert Plus software (see Supplementary Materials).

2.5. Computational Details

See Supplementary Materials.

3. Results and Discussion

For designing the synthetic procedures for **1** and **2**, we followed the same straightforward scheme—"source of Zn(II) + HPIBA + substituted pyridine"—expecting that the latter would play the roles of both the base, for the deprotonation of HPIBA, and the ligand, to complete the coordination environment of Zn. This idea worked well in the case of **1**, resulting in a pure phase, as shown by the PXRD data (see Supplementary Materials, Figures S1 and S2). At the same time, we found that the use of several substituted pyridines, namely 3-chloro, 2,5-diiodo, 2,6-dibromo, 2-iodo, 3-bromo, 2-bromo and 2-chloro derivatives, results in the formation of pure **2** with minor variations in yields (the nature of product was confirmed by means of element analysis and PXRD in all cases).

In **1**, the coordination environment of Zn(II) is tetrahedral (Figure 1). It consists of two 3,5-MePy ligands (Zn-N = 2.025 Å) and two PIBAs coordinated in monodentate mode (Zn-O = 1.950 Å).

The 3D system of halogen bonds in the structure of **1** is rather sophisticated (Figure 2). It involves O atoms of carboxylic groups in which each O interacts simultaneously with two iodine atoms. All 3-I and 5-I substituents participate in the formation of XB; the corresponding distances are 3.045 and 3.320 Å, which are much less than the sum of the related Bondi's van der Waals Radii (3.50 Å [28,29]; those are 87% and 94.8%, respectively). Additionally, there are I–I contacts (3.829–3.908 Å) involving 2-, 4- and 5-I atoms of PIBA ligands (Figure 3). This system of non-covalent interactions is very different from the one found in the similar complex [24] of Cu(II) with the same ligands due to the fundamentally different geometry of the coordination units.

Unlike in **1**, Zn(II) features hexa-coordination in the structure of **2** (Figure 4). There is one PIBA ligand (Zn-O = 2.018 Å), three DMF ligands (Zn-O = 2.034–2.084 Å) and one nitrate ligand; the latter is coordinated in bidentate mode (Zn-O = 2.116 and 2.473 Å, respectively).

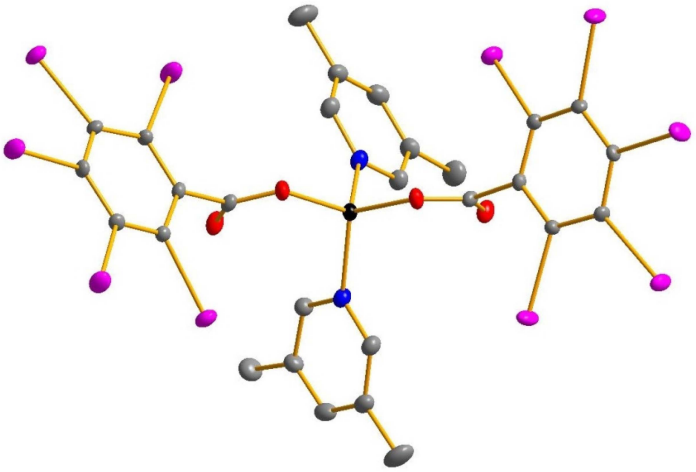

Figure 1. Structure of **1** (thermal ellipsoids, 50% probability). Here, and below: Zn—black, N—deep blue, C—grey, I—purple, O—red. H atoms are omitted for clarity.

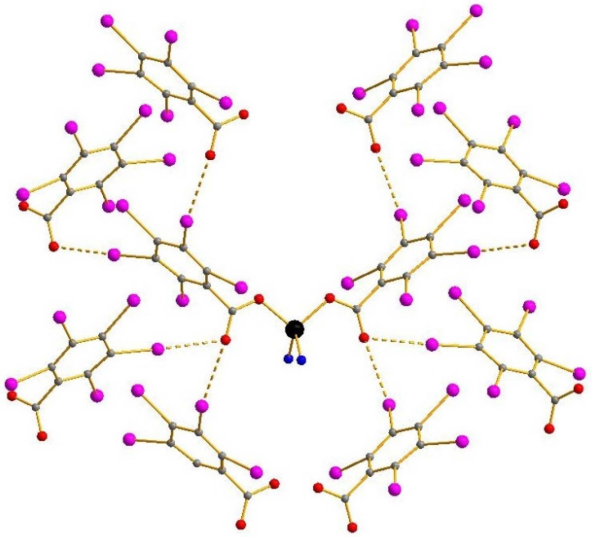

Figure 2. The system of I–O interactions (dashed) in the structure of **1**. Only N atoms of Py ligands are shown.

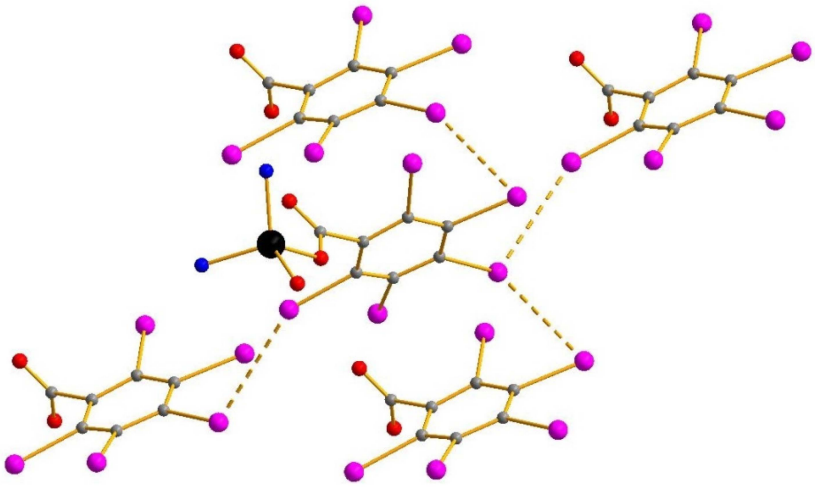

Figure 3. The system of I–I interactions (dashed) in the structure of **1**. Only N atoms of Py ligands are shown.

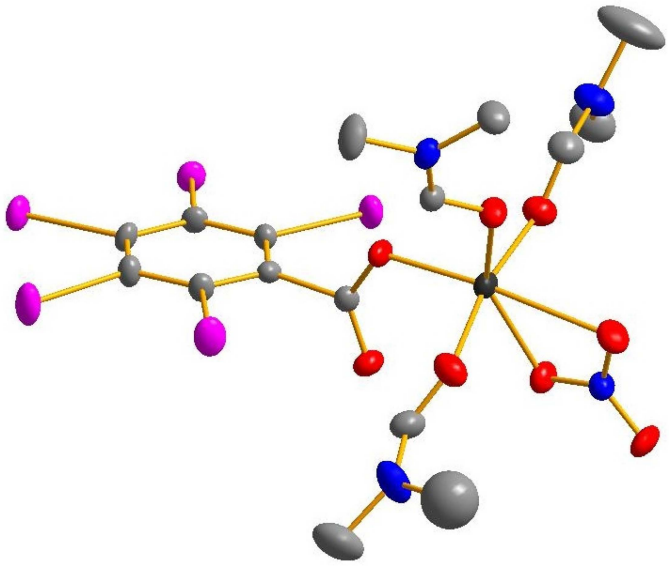

Figure 4. Structure of **2** (thermal ellipsoids, 50% probability).

Complex **2** also features multiple I–O halogen bonds, yielding a 3D structure (Figure 5). These involve O atoms of carboxylate groups (2.997–3.181 Å) and of nitrate ligands (3.079–3.129 Å, respectively). It must be noticed that XBs involving a nitrate anion or ligand are rather rare; as shown by the CSD data, there are fewer than 10 of such examples [30–35]. I–I non-covalent interactions are absent in this structure. Comparing the XBs in **1** and in relevant Cu(II) complexes which were reported by us recently [24], it can be seen that the lengths of non-covalent interactions are rather similar, likely corresponding to rather strong bonding.

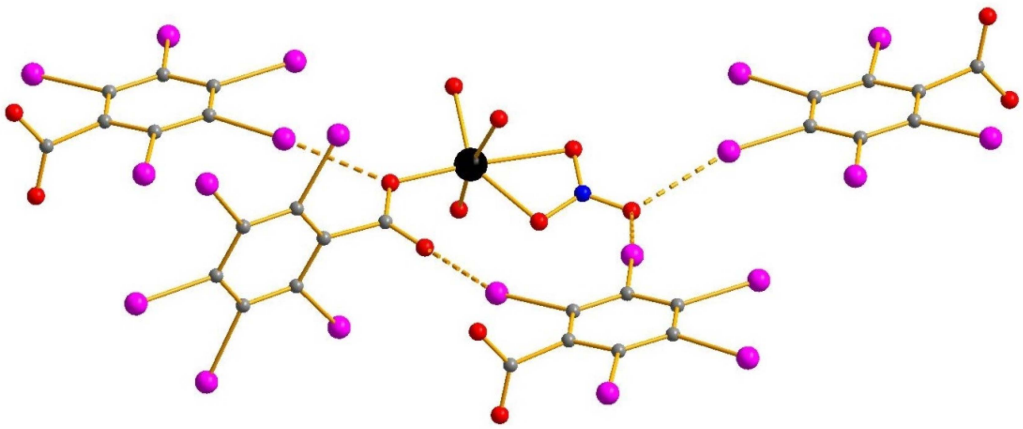

Figure 5. The system of I–O interactions (dashed) in the structure of **2**. Only O atoms of DMF ligands are shown.

To investigate the nature of non-covalent interactions in the structures of **1** and **2**, we used the approach which was previously used by us [36–40] and demonstrated its high efficiency: atomic coordinates were extracted from the XRD data and used for DFT calculations without optimization, followed by topological analysis of the electron density distribution (ωB97XD/DZP-DKH; see Supplementary Materials for details and visualization (Figures S3 and S4). The results are summarized in Table 2. It can be seen that the highest XB energies (5.1 kcal/mol) are comparable with those found in the structures of the corresponding Cu(II) complexes [24] and PIBA salts [20]).

The balance between the Lagrangian kinetic energy G(r) and potential energy density V(r) at the bond's critical points (3, –1) reveals [41] that a covalent contribution in the intermolecular interactions I–I and I–O in **1** and **2** is absent.

Table 2. Values of the density of all electrons ρ(**r**), Laplacian of electron density $\nabla^2\rho(\mathbf{r})$ and appropriate λ_2 eigenvalues; energy density H_b, potential energy density V(**r**), and Lagrangian kinetic energy G(**r**); and electron localization function ELF (a.u.) at the bond's critical points (3, –1) for intermolecular interactions in **1** and **2**, and their estimated strength E_{int} (kcal/mol).

Contact	Length	ρ (r)	$\nabla^2\rho$ (r)	$-\lambda_2$	H_b	$-$V (r)	G (r)	E_{int} *
				1				
I–I	3.908	0.007	0.029	0.007	0.002	0.004	0.006	1.7
I–I	3.829	0.009	0.033	0.009	0.001	0.006	0.007	2.6
I–O	3.321	0.008	0.035	0.008	0.002	0.005	0.007	2.1
I–O	3.045	0.015	0.054	0.015	0.001	0.011	0.012	4.7
				2				
I–O	3.181	0.011	0.047	0.011	0.002	0.008	0.010	3.4
I–O	3.129	0.012	0.047	0.012	0.001	0.009	0.010	3.8
I–O	3.079	0.014	0.053	0.014	0.002	0.010	0.012	4.3
I–O	2.997	0.017	0.060	0.017	0.002	0.012	0.014	5.1

* E_{int} = 0.88 ($-$V (**r**)) (this empirical correlation between the interaction energy and the potential energy density of electrons at the bond's critical points (3, –1) was specifically developed for non-covalent interactions involving bromine atoms) [42].

4. Conclusions

Our results confirm that PIBA can indeed be utilized as a ligand, and its complexes readily form halogen bonds in solid state. These findings can be applied for the preparation of other carboxylate complexes (this is a very large family of coordination compounds demonstrating fascinating structural diversity [43–48]); these could potentially be applicable in the design of contrast agents. Corresponding experiments are underway.

Supplementary Materials: The following supporting information can be downloaded at: https://www.mdpi.com/article/10.3390/inorganics10100151/s1, Figures S1 and S2. Comparison of experimental and calculated PXRD patterns for **1** and **2**; Computational details; Figures S3 and S4. Contour line diagrams of the Laplacian of electron density distribution, bond paths, and selected zero-flux surfaces, visualization of electron localization function and reduced density gradient analyses for intermolecular interactions I···I and I···O in **1** and **2**; Table S1. Cartesian atomic coordinates for model supramolecular associates.

Author Contributions: Conceptualization, S.A.A.; methodology, S.A.A. and A.S.N.; validation, A.S.N. and M.N.S., formal analysis, S.A.A., A.S.N. and M.N.S.; investigation, M.A.B. and A.S.N.; resources, S.A.A.; data curation, M.A.B. and A.S.N.; writing—original draft preparation, S.A.A.; writing—review and editing, M.N.S.; visualization, A.S.N. and S.A.A.; supervision, S.A.A.; project administration, S.A.A.; funding acquisition, S.A.A. All authors have read and agreed to the published version of the manuscript.

Funding: This research was funded by the Ministry of Science and Higher Education of the Russian Federation (121031700313-8). A.S.N. is grateful to the RUDN University Strategic Academic Leadership Program.

Data Availability Statement: Not applicable.

Acknowledgments: The authors thank Ilya V. Korolkov (NIIC SB RAS) for his assistance with PXRD experiments.

Conflicts of Interest: The authors declare no conflict of interest.

References

1. Yashkova, K.A.; Mel'nikov, S.N.; Nikolaevskii, S.A.; Shmelev, M.A.; Sidorov, A.A.; Kiskin, M.A.; Eremenko, I.L. Synthesis and structure of an nontrivial coordination polymer {[$Na_2Co(pfb)i_2$ $(H_2O)_8$](pfb)$_2$}$_n$ with pentafluorobenzoate anions. *J. Struct. Chem.* **2021**, *62*, 1378–1384. [CrossRef]
2. Shmelev, M.A.; Kuznetsova, G.N.; Dolgushin, F.M.; Voronina, Y.K.; Gogoleva, N.V.; Kiskin, M.A.; Ivanov, V.K.; Sidorov, A.A.; Eremenko, I.L. Influence of the Fluorinated Aromatic Fragments on the Structures of the Cadmium and Zinc Carboxylate Complexes Using Pentafluorobenzoates and 2,3,4,5-Tetrafluorobenzoates as Examples. *Russ. J. Coord. Chem.* **2021**, *47*, 127–143. [CrossRef]
3. Shmelev, M.A.; Gogoleva, N.V.; Kuznetsova, G.N.; Kiskin, M.A.; Voronina, Y.K.; Yakushev, I.A.; Ivanova, T.M.; Nelyubina, Y.V.; Sidorov, A.A.; Eremenko, I.L. Cd(II) and Cd(II)–Eu(III) Complexes with Pentafluorobenzoic Acid Anions and N-Donor Ligands: Synthesis and Structures. *Russ. J. Coord. Chem.* **2020**, *46*, 557–572. [CrossRef]
4. Shmelev, M.A.; Kiskin, M.A.; Voronina, J.K.; Babeshkin, K.A.; Efimov, N.N.; Varaksina, E.A.; Korshunov, V.M.; Taydakov, I.V.; Gogoleva, N.V.; Sidorov, A.A.; et al. Molecular and polymer ln_2m_2 (Ln = eu, gd, tb, dy; m = zn, cd) complexes with pentafluorobenzoate anions: The role of temperature and stacking effects in the structure; magnetic and luminescent properties. *Materials* **2020**, *13*, 5689. [CrossRef]
5. Utochnikova, V.V.; Grishko, A.; Vashchenko, A.; Goloveshkin, A.; Averin, A.; Kuzmina, N. Lanthanide Tetrafluoroterephthalates for Luminescent Ink-Jet Printing. *Eur. J. Inorg. Chem.* **2017**, *2017*, 5635–5639. [CrossRef]
6. Kalyakina, A.S.; Utochnikova, V.V.; Bushmarinov, I.S.; Le-Deygen, I.M.; Volz, D.; Weis, P.; Schepers, U.; Kuzmina, N.P.; Bräse, S. Lanthanide Fluorobenzoates as Bio-Probes: A Quest for the Optimal Ligand Fluorination Degree. *Chem. A Eur. J.* **2017**, *23*, 14944–14953. [CrossRef]
7. Mironova, A.D.; Mikhaylov, M.A.; Maksimov, A.M.; Brylev, K.A.; Gushchin, A.L.; Stass, D.V.; Novikov, A.S.; Eltsov, I.V.; Abramov, P.A.; Sokolov, M.N. Phosphorescent Complexes of $\{Mo_6I_8\}^{4+}$ and $\{W_6I_8\}^{4+}$ with Perfluorinated Aryl Thiolates featuring Unusual Molecular Structures. *Eur. J. Inorg. Chem.* **2022**, *2022*, e202100890. [CrossRef]
8. Rogozhin, A.F.; Silantyeva, L.I.; Yablonskiy, A.N.; Andreev, B.A.; Grishin, I.D.; Ilichev, V.A. Near infrared luminescence of Nd, Er and Yb complexes with perfluorinated 2-mercaptobenzothiazolate and phosphine oxide ligands. *Opt. Mater.* **2021**, *118*, 111241. [CrossRef]
9. Silantyeva, L.I.; Ilichev, V.A.; Shavyrin, A.S.; Yablonskiy, A.N.; Rumyantcev, R.V.; Fukin, G.K.; Bochkarev, M.N. Unexpected findings in a simple metathesis reaction of europium and ytterbium diiodides with perfluorinated mercaptobenzothiazolates of alkali metals. *Organometallics* **2020**, *39*, 2972–2983. [CrossRef]
10. Bhat, S.A.; Iftikhar, K. Synthesis and NIR photoluminescence studies of novel Yb(III) complexes of asymmetric perfluoryl β-diketone. *J. Lumin.* **2019**, *208*, 334–341. [CrossRef]
11. Balashova, T.V.; Burin, M.E.; Ilichev, V.A.; Starikova, A.A.; Marugin, A.V.; Rumyantcev, R.V.; Fukin, G.K.; Yablonskiy, A.N.; Andreev, B.A.; Bochkarev, M.N. Features of the molecular structure and luminescence of rare-earth metal complexes with perfluorinated (Benzothiazolyl)phenolate Ligands. *Molecules* **2019**, *24*, 2376. [CrossRef]
12. Abramov, P.A.; Brylev, K.A.; Vorob'ev, A.Y.; Gatilov, Y.V.; Borodkin, G.I.; Kitamura, N.; Sokolov, M.N. Emission tuning in Re(I) complexes: Expanding heterocyclic ligands and/or introduction of perfluorinated ligands. *Polyhedron* **2017**, *137*, 231–237. [CrossRef]
13. Kalyakina, A.S.; Utochnikova, V.V.; Bushmarinov, I.S.; Ananyev, I.V.; Eremenko, I.L.; Volz, D.; Rönicke, F.; Schepers, U.; Van Deun, R.; Trigub, A.L.; et al. Highly Luminescent, Water-Soluble Lanthanide Fluorobenzoates: Syntheses, Structures and Photophysics, Part I: Lanthanide Pentafluorobenzoates. *Chem. A Eur. J.* **2015**, *21*, 17921–17932. [CrossRef]
14. Claus, A.; Bücher, A.W. Zur Kenntniss der Chlorbenzoësäuren. *Ber. Dtsch. Chem. Ges.* **1887**, *20*, 1621–1627. [CrossRef]
15. Ballester, M.; Castañer, J.; Riera, J.; Tabernero, I. Synthesis and Chemical Behavior of Perchlorophenylacetylene. *J. Org. Chem.* **1986**, *51*, 1413–1419. [CrossRef]
16. Ozaki, K.; Okuno, T. Crystal polymorphs and ab initio calculation of 2,3,4,5,6-pentachlorobenzoic acid. *J. Mol. Struct.* **2018**, *1173*, 959–963. [CrossRef]
17. Sharutin, V.V.; Sharutina, O.K. Synthesis and structure of triphenylbismuth bis(pentachlorobenzoate). *Russ. J. Inorg. Chem.* **2014**, *59*, 558–560. [CrossRef]
18. Mattern, D.L. Direct aromatic periodination. *J. Org. Chem.* **1984**, *49*, 3051–3053. [CrossRef]
19. deKrafft, K.E.; Xie, Z.; Cao, G.; Tran, S.; Ma, L.; Zhou, O.; Lin, W. Iodinated Nanoscale Coordination Polymers as Potential Contrast Agents for Computed Tomography. *Angew. Chem. Int. Ed.* **2009**, *48*, 9901–9904. [CrossRef]
20. Adonin, S.A.; Bondarenko, M.A.; Novikov, A.S.; Abramov, P.A.; Sokolov, M.N.; Fedin, V.P. Halogen bonding in the structures of pentaiodobenzoic acid and its salts. *CrystEngComm* **2019**, *21*, 6666–6670. [CrossRef]
21. Bertani, R.; Sgarbossa, P.; Venzo, A.; Lelj, F.; Amati, M.; Resnati, G.; Pilati, T.; Metrangolo, P.; Terraneo, G. Halogen bonding in metal–organic–supramolecular networks. *Coord. Chem. Rev.* **2010**, *254*, 677–695. [CrossRef]
22. Li, B.; Zang, S.-Q.; Wang, L.-Y.; Mak, T.C.W. Halogen bonding: A powerful, emerging tool for constructing high-dimensional metal-containing supramolecular networks. *Coord. Chem. Rev.* **2016**, *308*, 1–21. [CrossRef]
23. Mahmudov, K.T.; Kopylovich, M.N.; Guedes da Silva, M.F.C.; Pombeiro, A.J.L. Non-covalent interactions in the synthesis of coordination compounds: Recent advances. *Coord. Chem. Rev.* **2017**, *345*, 54–72. [CrossRef]

24. Bondarenko, M.A.; Abramov, P.A.; Novikov, A.S.; Sokolov, M.N.; Adonin, S.A. Cu(II) pentaiodobenzoate complexes: "super heavy carboxylates" featuring strong halogen bonding. *Polyhedron* **2022**, *214*, 115644. [CrossRef]
25. Sheldrick, G.M. SHELXT—Integrated space-group and crystal-structure determination. *Acta Crystallogr. Sect. A Found. Adv.* **2015**, *71*, 3–8. [CrossRef]
26. Sheldrick, G.M. Crystal structure refinement with SHELXL. *Acta Crystallogr. Sect. C Struct. Chem.* **2015**, *71*, 3–8. [CrossRef]
27. Hübschle, C.B.; Sheldrick, G.M.; Dittrich, B. ShelXle: A Qt graphical user interface for SHELXL. *J. Appl. Crystallogr.* **2011**, *44*, 1281–1284. [CrossRef]
28. Bondi, A. van der Waals Volumes and Radii of Metals in Covalent Compounds. *J. Phys. Chem.* **1966**, *70*, 3006–3007. [CrossRef]
29. Mantina, M.; Chamberlin, A.C.; Valero, R.; Cramer, C.J.; Truhlar, D.G. Consistent van der Waals Radii for the Whole Main Group. *J. Phys. Chem. A* **2009**, *113*, 5806–5812. [CrossRef]
30. Takezawa, H.; Murase, T.; Resnati, G.; Metrangolo, P.; Fujita, M. Halogen-Bond-Assisted Guest Inclusion in a Synthetic Cavity. *Angew. Chem. Int. Ed.* **2015**, *54*, 8411–8414. [CrossRef]
31. Decato, D.A.; Riel, A.M.S.; Berryman, O.B. Anion influence on the packing of 1,3-bis(4-ethynyl-3-iodopyridinium)-benzene halogen bond receptors. *Crystals* **2019**, *9*, 522. [CrossRef] [PubMed]
32. Amendola, V.; Bergamaschi, G.; Boiocchi, M.; Fusco, N.; La Rocca, M.V.; Linati, L.; Lo Presti, E.; Mella, M.; Metrangolo, P.; Miljkovic, A. Novel hydrogen- and halogen-bonding anion receptors based on 3-iodopyridinium units. *RSC Adv.* **2016**, *6*, 67540–67549. [CrossRef]
33. Chandran, S.K.; Thakuria, R.; Nangia, A. Silver(I) complexes of N-4-halophenyl-N′-4-pyridyl ureas. Isostructurality, urea···nitrate hydrogen bonding, and Ag···halogen interaction. *CrystEngComm* **2008**, *10*, 1891–1898. [CrossRef]
34. Zisti, F.; Tehrani, A.A.; Alizadeh, R.; Abbasi, H.; Morsali, A.; Eichhorn, S.H. Synthesis and structural characterization of three nano-structured Ag(I) coordination polymers; Syntheses, characterization and X-ray crystal structural analysis. *J. Solid State Chem.* **2019**, *271*, 29–39. [CrossRef]
35. Powell, J.; Horvath, M.J.; Lough, A. Silver-iodocarbon complexes: Crystal structures of eight compounds obtained from the reactions of $AgPF_6$ or $AgNO_3$ with CH_2I_2, $I(CH_2)_3I$ and simple aryl iodides. *J. Chem. Soc. Dalt. Trans.* **1996**, 1669–1677. [CrossRef]
36. Melekhova, A.A.; Novikov, A.S.; Dubovtsev, A.Y.; Zolotarev, A.A.; Bokach, N.A. Tris(3,5-dimethylpyrazolyl)methane copper(I) complexes featuring one disubstituted cyanamide ligand. *Inorg. Chim. Acta* **2019**, *484*, 69–74. [CrossRef]
37. Bulatova, M.; Melekhova, A.A.; Novikov, A.S.; Ivanov, D.M.; Bokach, N.A. Redox reactive $(RNC)Cu^{II}$ species stabilized in the solid state via halogen bond with I_2. *Z. Krist. Cryst. Mater.* **2018**, *233*, 371–377. [CrossRef]
38. Bokach, N.A.; Suslonov, V.V.; Eliseeva, A.A.; Novikov, A.S.; Ivanov, D.M.; Dubovtsev, A.Y.; Kukushkin, V.Y.; Kukushkin, V.Y. Tetrachloroplatinate(ii) anion as a square-planar tecton for crystal engineering involving halogen bonding. *CrystEngComm* **2020**, *22*, 4180–4189.
39. Eliseeva, A.A.; Ivanov, D.M.; Novikov, A.S.; Kukushkin, V.Y. Recognition of the π-hole donor ability of iodopentafluorobenzene-a conventional σ-hole donor for crystal engineering involving halogen bonding. *CrystEngComm* **2019**, *21*, 616–628. [CrossRef]
40. Ivanov, D.M.; Kinzhalov, M.A.; Novikov, A.S.; Ananyev, I.V.; Romanova, A.A.; Boyarskiy, V.P.; Haukka, M.; Kukushkin, V.Y. $H_2C(X)–X\cdots X^-$ (X = Cl, Br) Halogen Bonding of Dihalomethanes. *Cryst. Growth Des.* **2017**, *17*, 1353–1362. [CrossRef]
41. Espinosa, E.; Alkorta, I.; Elguero, J.; Molins, E. From weak to strong interactions: A comprehensive analysis of the topological and energetic properties of the electron density distribution involving X–H···F–Y systems. *J. Chem. Phys.* **2002**, *117*, 5529–5542. [CrossRef]
42. Bartashevich, E.V.; Tsirelson, V.G. Interplay between non-covalent interactions in complexes and crystals with halogen bonds. *Russ. Chem. Rev.* **2014**, *83*, 1181–1203. [CrossRef]
43. Goldberg, A.E.; Kiskin, M.A.; Nikolaevskii, S.A.; Zorina-Tikhonova, E.N.; Aleksandrov, G.G.; Sidorov, A.A.; Eremenko, I.L. Structural influence of the substituent in carboxylate anion on example of α- And β-naphthoate complexes of Co(II), Ni(II), Cu(II), and Zn(II). *Russ. J. Coord. Chem.* **2015**, *41*, 182–188. [CrossRef]
44. Nikolaevskii, S.A.; Kiskin, M.A.; Starikova, A.A.; Efimov, N.N.; Sidorov, A.A.; Novotortsev, V.M.; Eremenko, I.L. Binuclear nickel(II) complexes with 3,5-di-tert-butylbenzoate and 3,5-di-tert-butyl-4-hydroxybenzoate anions and 2,3-lutidine: The synthesis, structure, and magnetic properties. *Russ. Chem. Bull.* **2016**, *65*, 2812–2819. [CrossRef]
45. Yambulatov, D.S.; Nikolaevskii, S.A.; Lutsenko, I.A.; Kiskin, M.A.; Shmelev, M.A.; Bekker, O.B.; Efimov, N.N.; Ugolkova, E.A.; Minin, V.V.; Sidorov, A.A.; et al. Copper(II) Trimethylacetate Complex with Caffeine: Synthesis, Structure, and Biological Activity. *Russ. J. Coord. Chem.* **2020**, *46*, 772–778. [CrossRef]
46. Yin, W.-D.; Li, G.-L.; Liu, M.-N.; Du, G.-J.; Shao, Y.; Liu, G.-Z. Syntheses, Structures, and Magnetic Properties of Two Cu(II) Coordination Polymers Based on 4-Nitrophthalic Acid. *Russ. J. Inorg. Chem.* **2021**, *66*, 2077–2083. [CrossRef]
47. Nikolaevskii, S.A.; Yambulatov, D.S.; Starikova, A.A.; Sidorov, A.A.; Kiskin, M.A.; Eremenko, I.L. Molecular Structure and Photoluminescence Behavior of the Zn(II) Carboxylate Complex with Pyrazino [2,3-f][1,10]phenanthroline. *Russ. J. Coord. Chem.* **2020**, *46*, 260–267. [CrossRef]
48. Dorofeeva, V.N.; Pavlishchuk, A.V.; Kiskin, M.A.; Efimov, N.N.; Minin, V.V.; Gavrilenko, K.S.; Kolotilov, S.V.; Pavlishchuk, V.V.; Eremenko, I.L. Generation of Long-Lived Phenoxyl Radical in the Binuclear Copper(II) Pivalate Complex with 2,6-Di-tert-butyl-4-(3,5-bis(4-pyridyl)pyridyl)phenol. *Russ. J. Coord. Chem.* **2022**, *48*, 422–429. [CrossRef]